Journal of Experimental Marine Biology and Ecology 451 (2014) 44–54

Contents lists available at ScienceDirect

Journal of Experimental Marine Biology and Ecology

journal homepage: www.elsevier.com/locate/jembe

Photophysiological responses of Southern Ocean phytoplankton to changes in CO_2 concentrations: Short-term versus acclimation effects ☆

Scarlett Trimborn [a,*], Silke Thoms [a], Katherina Petrou [b], Sven A. Kranz [c], Björn Rost [a]

[a] Alfred Wegener Institute for Polar and Marine Research, Am Handelshafen 12, 27570 Bremerhaven, Germany
[b] University of Technology, Plant Functional Biology and Climate Change Cluster, Department of Environmental Sciences, PO Box 123, Broadway, NSW 2007, Sydney, Australia
[c] Princeton University, Department of Geosciences, Princeton, NJ 08544, USA

ARTICLE INFO

Article history:
Received 31 July 2013
Received in revised form 4 November 2013
Accepted 7 November 2013
Available online 5 December 2013

Keywords:
Dark respiration
Effective quantum yield of PSII
Electron transport rates
Mehler reaction
Ocean acidification
Photophysiology

ABSTRACT

The present study examines how different pCO_2 acclimations affect the CO_2- and light-dependence of photophysiological processes and O_2 fluxes in four Southern Ocean (SO) key phytoplankton species. We grew *Chaetoceros debilis* (Cleve), *Pseudo-nitzschia subcurvata* (Hasle), *Fragilariopsis kerguelensis* (O'Meara) and *Phaeocystis antarctica* (Karsten) under low (160 μatm) and high (1000 μatm) pCO_2. The CO_2- and light-dependence of fluorescence parameters of photosystem II (PSII) were determined by means of a fluorescence induction relaxation system (FIRe). In all tested species, nonphotochemical quenching (NPQ) is the primary photoprotection strategy in response to short-term exposure to high light or low CO_2 concentrations. In *C. debilis* and *P. subcurvata*, PSII connectivity (p) and functional absorption cross-sections of PSII in ambient light (σ'_{PSII}) also contributed to photoprotection while changes in re-oxidation times of Q_a acceptor (τ_{Qa}) were more significant in *F. kerguelensis*. The latter was also the only species being responsive to high acclimation pCO_2, as these cells had enhanced relative electron transport rates (rETRs) and σ'_{PSII} while τ_{Qa} and p were reduced under short-term exposure to high irradiance. Low CO_2-acclimated cells of *F. kerguelensis* and all pCO_2 acclimations of *C. debilis* and *P. subcurvata* showed dynamic photoinhibition with increasing irradiance. To test for the role and presence of the Mehler reaction in *C. debilis* and *P. subcurvata*, the light-dependence of O_2 fluxes was estimated using membrane inlet mass spectrometry (MIMS). Our results show that the Mehler reaction is absent in both species under the tested conditions. We also observed that dark respiration was strongly reduced under high pCO_2 in *C. debilis* while it remained unaltered in *P. subcurvata*. Our study revealed species-specific differences in the photophysiological responses to pCO_2, both on the acclimation as well as the short-term level.

Abbreviations: a^*_{PSII}, optical cross section for photosystem II; α, maximum light-use efficiency; ATP, adenosine triphosphate; CCM, carbon concentrating mechanism; cf, conversion factor; Chl *a*, chlorophyll *a*; C_i, inorganic carbon; CO_2, carbon dioxide; DBS, dextran-bound sulfonamide (inhibitor for eCA); DIC, dissolved inorganic carbon; eCA, extracellular carbonic anhydrase; ETR, electron transport rate; FIRe, fluorescence induction relaxation system; F_0, minimum fluorescence; F'_0, light-adapted minimum fluorescence; F_m, maximum fluorescence; F'_m, light-adapted maximum fluorescence; F_v/F_m, maximum quantum yield of photochemistry in photosystem II according to Genty et al. (1989); F'_q/F'_m, effective quantum yield of photochemistry in photosystem II; HCO_3^-, bicarbonate; HEPES, 2-[4-(2-Hydroxyethyl)-1-piperazinyl]ethanesulfonic acid; I, irradiance; I_k, light acclimation index; J, connectivity parameter according to Lavergne and Trissl (1995); MIMS, membrane inlet mass spectrometry; MTF, multiple turnover flash; NADH, nicotinamide adenine dinucleotide; NADPH, nicotinamide adenine dinucleotide phosphate; $NaHCO_3$, sodium bicarbonate; NPQ, non-photochemical quenching; O_2, oxygen; p, connectivity between photosystem II according to Joliot and Joliot (1964); p', connectivity between photosystem II in ambient light; pCO_2, carbon dioxide partial pressure; Φ_{PSII}, quantum yield of photochemistry in photosystem II according to Lavergne and Trissl (1995); Φ^m_{PSII}, maximum quantum yield of photochemistry in photosystem II according to Lavergne and Trissl (1995); PQ, plastoquinone; PSI, photosystem I; PSII, photosystem II; q, overall fraction of open photosystem II units; rETR, relative electron transport rate; RuBisCO, ribulose-1,5-bisphosphate carboxylase–oxygenase; σ_{PSII}, functional absorption cross section of photosystem II; σ'_{PSII}, functional absorption cross section of photosystem II in ambient light; SO, Southern Ocean; STF, single turnover flash; τ_{Qa}, re-oxidation time of the Q_a acceptor; τ'_{Qa}, re-oxidation time of the Q_a acceptor in ambient light; V_{max}, light-saturated net rate of photosynthesis.

* Corresponding author at: Alfred Wegener Institute, Helmholtz Centre for Polar and Marine Research, Am Handelshafen 12 (E-2010), 27570 Bremerhaven, Germany. Tel.: +49 471 4831 1038; fax: +49 471 4831 2020.
E-mail address: scarlett.trimborn@awi.de (S. Trimborn).

0022-0981/$ – see front matter © 2013 The Authors. Published by Elsevier B.V. All rights reserved.
http://dx.doi.org/10.1016/j.jembe.2013.11.001

1. Introduction

By the end of 2100, the ongoing anthropogenic emissions of carbon dioxide (CO_2) will likely have increased atmospheric CO_2 concentrations from ~390 μatm to >750 μatm (IPCC report I, 2007). Biogeochemical models for the ocean indicate that the rise in atmospheric CO_2 levels will affect seawater carbonate chemistry by decreasing the current seawater pH of ~8.1 by 0.3 units (Feely et al., 2009). Next to this reduction in pH, higher CO_2 concentrations will also lead to reduced carbonate ion concentrations and saturation states, a phenomenon commonly referred to as 'ocean acidification' (Orr et al., 2005). Due to the high solubility of CO_2 in cold waters, these changes in carbonate chemistry will be most pronounced in polar waters. The Southern Ocean (SO) ecosystem strongly influences the marine carbon cycle and has a great potential to affect atmospheric CO_2 concentrations (Sigman et al., 2010). Although SO phytoplankton are major drivers of global carbon cycling accounting for ~2 Pg C of annual primary production (Arrigo et al., 2008), the potential effects of ocean acidification on the physiology and ecology of SO phytoplankton are still not well understood. There is evidence that high pCO_2 differently affects SO phytoplankton growth (Boelen et al., 2011; Hoogstraten et al., 2012a, 2012b; Ihnken et al., 2011a; Trimborn et al., 2013) potentially causing changes in the community structure (Feng et al., 2010; Tortell et al., 2008). For natural phytoplankton assemblages of the China Sea, it was observed that high pCO_2 in conjunction with high light exposure can reduce their primary productivity and increase light stress (Gao et al., 2012). A higher susceptibility for photoinhibition at high pCO_2 was also indicated in different temperate phytoplankton species (McCarthy et al., 2012; Wu et al., 2010; Yang and Gao, 2012). In this context, it is particularly surprising that most central processes like the photophysiology of SO phytoplankton have hardly been studied in the context of ocean acidification research.

Thus far, studies on the photophysiology of SO phytoplankton mainly focused on the effect of different light levels (Arrigo et al., 2010; Kropuenske et al., 2009; Robinson et al., 1997; Van Leuwe et al., 2005). Next to the adjustment of cellular pigment composition and concentration (Arrigo et al., 2010; Van Leuwe et al., 2005), the photoacclimation strategy of polar phytoplankton is to adjust photosystem II (PSII) reaction centers through changing the size of the effective absorption cross-section (σ_{PSII}) rather than the number of PSII reaction centers per cell (Kropuenske et al., 2010; Robinson et al., 1997). Phytoplankton can also alter the PSII connectivity (p) allowing the redistribution of excitons from closed to open PSII providing a more or less efficient use of light (Ihnken et al., 2011b). Regarding the impact of pCO_2 on photophysiology, Spalding et al. (1984) reported an increase in σ_{PSII} in *Chlamydomonas reinhardtii* when grown at 5% CO_2. In the Antarctic diatom *Chaetoceros brevis*, however, Boelen et al. (2011) observed no effect by elevated pCO_2 (750 μatm) on either pigment content and composition or the activity of the carbon-fixing enzyme Ribulose-1,5-bisphosphate carboxylase–oxygenase (RubisCO).

Next to light, photosynthesis requires CO_2 as the substrate of RubisCO and its availability may also affect the photophysiology of the cells. To avoid limitations arising from low CO_2 supply and the low CO_2 affinities of RubisCO, most phytoplankton operate so-called carbon concentrating mechanisms (CCMs; Reinfelder, 2011). Trimborn et al. (2013) demonstrated that SO phytoplankton species have diverse and highly efficient CCMs, which were often constitutively expressed independent of the acclimation pCO_2. The operation of a CCM is an energy-requiring process and is therefore strongly dependent on light (Raven and Lucas, 1985). In fact, carbon acquisition and subsequent fixation consume the largest share of the ATP and NADPH produced in the light reaction of photosynthesis. As photosynthesis cannot go faster than either the carboxylase activity or the electron transport rate and considering the large variability in irradiance and CO_2 in the natural environment, phytoplankton require high flexibility to adjust their CCM as well as their photosynthetic apparatus for optimal use. It has been suggested that under low CO_2 conditions, not only the cycling of electrons around photosystem I (PSI; Spalding et al., 1984), but also indirectly the Mehler reaction, the photoreduction of O_2, supplies ATP required for the operation of the CCM (Raven and Beardall, 1981; Sültemeyer et al., 1993). High pCO_2, on the other hand, may reduce costs for CCM activity and thus the energy demand (Kranz et al., 2010), all of which may feedback on photophysiology. Until now, information on these processes and their sensitivity to ocean acidification is lacking for SO phytoplankton.

The exposure of phytoplankton cells to high irradiances requires the dissipation of excess energy to prevent damage of PSII. To this end, phytoplankton possess photoprotective mechanisms such as non-photochemical quenching (NPQ) and the electron cycling around the PSI and/or PSII (Prasil et al., 1996) that respond within time scales of seconds to minutes. Xanthophyll-cycle-dependent NPQ has been observed in both *Phaeocystis antarctica* and SO diatoms (Boelen et al., 2011; Kropuenske et al., 2009; Mills et al., 2010; Petrou et al., 2011) and involves the enzymatic removal of the epoxy group of the carotenoid diadinoxanthin to diatoxanthin. This process is triggered by a decrease in the pH of the thylakoid lumen and represents a central mechanism to prevent photoinhibition under excessive light. The Mehler reaction can also act as a photoprotective mechanism in phytoplankton (Raven and Beardall, 1981). Kranz et al. (2010) observed Mehler activity in the cyanobacterium *Trichdesmium*, which was acclimated to low pCO_2 combined with high light, but this process was absent under high pCO_2. In the temperate diatom *Chaetoceros muelleri*, increasing pCO_2 was found to enhance relative electron transport rates (rETRs) under saturating light, suggesting that higher rETRs were enabled because of elevated CO_2 fixation rates by RubisCO (Ihnken et al., 2011a, 2011b). McCarthy et al. (2012) also observed higher carboxylation rates with increasing pCO_2 in two temperate diatom strains of *Thalassiosira pseudonana*. In the same study, the tested species were nonetheless found to be more susceptible to photoinhibition and to have a higher capacity for PSII repair at elevated pCO_2. Whether Antarctic phytoplankton may respond in a similar way is not yet resolved.

The present study examines how the acclimation pCO_2 affects photophysiological processes and O_2 fluxes of four SO key phytoplankton species in response to short-term changes in CO_2 or irradiance. To this end, *Chaetoceros debilis*, *Pseudo-nitzschia subcurvata*, *Fragilariopsis kerguelensis* and *P. antarctica* were acclimated to 160 and 1000 μatm pCO_2. The CO_2- and light-dependence of chlorophyll *a* fluorescence were assessed using a fluorescence induction relaxation system (FIRe; Satlantic, Canada). Also, the light-dependence of O_2 fluxes (gross and net photosynthesis as well as O_2 uptake in the light and in the dark) was determined in *C. debilis* and *P. subcurvata* according to the method of Peltier and Thibault (1985) by means of membrane inlet mass spectrometry (MIMS).

2. Material and methods

2.1. Culture conditions and carbonate chemistry

Semi-continuous cultures of the diatom species *C. debilis* (Polarstern expedition 'EIFEX' ANT-XXI/3, In-Patch, 2004, 49°36 S Lat, 02°05 E Long, isolated by Philipp Assmy), *P. subcurvata* (Polarstern expedition ANT-XXI/4 in April 2004 at 49° S Lat, 02° E Long, isolated by Philipp Assmy) and *F. kerguelensis* (Polarstern expedition ANT-XXIV/2 in 2008 at 64° S Lat, 0° E Long, isolated by Philipp Assmy) and the flagellate *P. antarctica* (solitary cells isolated by P. Pendoley in March 1992 at 68°39 S, 72°21) were grown at 3 °C in sterile-filtered (0.2 μm) unbuffered Antarctic seawater (salinity 33.9 psu). The seawater was enriched with trace metals and vitamins according to F/2 medium (Guillard and Ryther, 1962). Nitrate and phosphate were added in concentrations of 100 and 6.25 μmol L^{-1}, respectively, reflecting the Redfield N:P ratio of 16:1 (Redfield, 1958). Experiments were carried out using a light:dark cycle of 16:8 h at an incident light intensity of

90 μmol photons m^{-2} s^{-1}. Cultures were continuously bubbled through a frit with humidified air of CO_2 partial pressures (pCO_2) of 160 and 1000 μatm (low and high pCO_2). CO_2 gas mixtures were generated with gas-mixing pumps (Woesthoff GmbH, Bochum, Germany), using CO_2-free air (Nitrox CO_2 RP280, Domnick Hunter ltd., Willich, Germany) and pure CO_2 (Air Liquide Deutschland ltd., Germany). As cultures were diluted regularly with pre-equilibrated medium, cells stayed in the mid-exponential growth phase and carbonate chemistry remained constant. The pH was 8.47 ± 0.02 and 7.77 ± 0.03 for the low and high pCO_2 acclimations, respectively. The pH was measured on a daily basis using a pH–ion-meter (WTW, model pMX 3000/pH, Weilheim, Germany). Alkalinity samples were taken from the filtrate (Whatman GFF filter, ~0.6 mm), stored in 300 mL borosilicate flasks at 4 °C, and measured by potentiometric titration (Brewer et al., 1986). Total alkalinity (TA) was calculated from linear Gran Plots (Gran, 1952). The carbonate system was calculated from TA, pH, silicate, phosphate, temperature, and salinity using the CO2Sys program (Pierrot et al., 2006). The parameters of the carbonate system for the respective treatments are given in Table 1. Cells were acclimated to experimental conditions for at least 2 weeks prior to sampling. After acclimation, growth rates of *C. debilis* were 0.59 ± 0.11 d^{-1} under low pCO_2 and 0.96 ± 0.16 d^{-1} under high pCO_2. Growth rates of *P. subcurvata* and *P. antarctica* were not affected by the acclimation pCO_2, being 0.87 ± 0.20 d^{-1} and 0.41 ± 0.05 d^{-1}, respectively. Due to problems with the cell count samples of *F. kerguelensis*, growth rates could not be determined for this species.

2.2. CO_2- or light-dependent chlorophyll a fluorescence

Using a fluorescence induction relaxation system (FIRe; Satlantic, Canada), chlorophyll *a* fluorescence was assessed in cells that were either exposed to increasing dissolved inorganic carbon (DIC) concentrations (50, 100, 250, 500, 1000, 2500 μmol L^{-1} DIC at the acclimation irradiance of 90 μmol photons m^{-2} s^{-1}) or to increasing irradiance levels (35, 90, 130, 180, 400, 765, 1425 μmol photons m^{-2} s^{-1} at acclimation DIC concentrations of ≥2000 μmol L^{-1}). CO_2- or light-dependent measurements were performed with all tested species acclimated to low and high pCO_2. Only for *P. antarctica*, light-dependent chlorophyll *a* fluorescence measurements were not conducted.

To this end, cells were harvested by gentle filtration over a 3 μm membrane filter (Isopore, Millipore) and then washed with initially CO_2-free F/2 medium buffered with 50 mmol L^{-1} 2-[4-(2-Hydroxyethyl)-1-piperazinyl]ethanesulfonic acid (HEPES, pH 7.8 or 8.1, depending on the treatment). Cells were then transferred to a temperature-controlled cuvette, which was set to the growth temperature of 3 °C. Chlorophyll *a* fluorescence was measured in consecutive light–dark intervals of 10 min each. In the case of the CO_2-dependent assay, the respective DIC concentration was added in form of $NaHCO_3$ solutions (0.1 or 1 M) to the buffered assay medium at the beginning of the dark interval. Depending on equilibration time of the respective DIC addition, light and dark intervals during this assay lasted between 10 min and 15 min. At the end of the dark phase, cells were then exposed to a strong saturating flash (140 μs Single Turnover Flash, STF), which was applied in order to cumulatively saturate PSII. Then a relaxation period (60 μs) of 60 weak modulated light pulses followed to record the relaxation kinetics of fluorescence yield. Afterwards a longer saturating pulse (240 ms Multiple Turnover Flash, MTF) was applied in order to saturate PSII as well as the PQ pool. From this measurement, the minimum (F_o) of the STF and maximum (F_m) fluorescence of the MTF was determined. Using these two parameters, the maximum quantum yield of photochemistry in PSII (F_v/F_m) was calculated according to the equation $(F_m - F_o) / F_m$.

During the light intervals, cells were exposed either to 90 μmol photons m^{-2} s^{-1} (CO_2-dependent assay) or to increasing irradiance levels (light-dependent assay). From these measurements, the light-adapted minimum (F) of the STF and maximum (F'_m) fluorescence of the MTF were estimated at the end of the respective light intervals. The effective quantum yield of photochemistry in open reaction centers of PSII (F'_q/F'_m) was derived according to the equation $(F'_m - F) / F'_m$ (Genty et al., 1989). From the STF, the functional absorption cross section of PSII in ambient light (σ'_{PSII}) was assessed. Relative electron transport rates (rETRs) were calculated as the product of effective quantum yield and applied irradiance. Using the Stern–Volmer equation, non-photochemical quenching (NPQ) of chlorophyll *a* fluorescence was calculated as $F_m / F'_m - 1$. During both dark and light intervals, the energy transfer between PSII units (i.e. connectivity factor, p and p', respectively) and the time constant for the electron transport on the acceptor side of PSII (i.e. re-oxidation of the Q_a acceptor, τ_{Qa} and τ'_{Qa}, respectively) were recorded using the FIRe system. Re-oxidation times τ_{Qa} and τ'_{Qa} were calculated according to Kolber et al. (1998). Values of photosynthetic parameters were derived using the FIRePro software provided by Satlantic Inc. (v. 1.20., Halifax, Canada). At the end of each assay, the applied irradiance levels were measured in the cuvette within the concentrated cell suspension using a LI-1400 datalogger (Li-Cor, Lincoln, NE, USA) with a 4π-sensor (Walz, Effeltrich, Germany).

2.3. Light-dependent photosynthetic O_2 evolution and O_2 uptake

Using membrane inlet mass spectrometry (MIMS), rates of O_2 production and O_2 uptake were determined in *C. debilis* and *P. subcurvata* acclimated to low and high pCO_2. Cells were harvested by gentle filtration over a 3 μm membrane filter (Isopore, Millipore) and subsequently washed with F/2 medium buffered with 50 mmol L^{-1} HEPES (pH 8.0). In addition to this, the respective medium was purged with N_2 for 1.5 to 2 h and spiked with $^{18}O_2$ before cells were harvested. The culture medium was then exchanged stepwise with the $^{18}O_2$-enriched assay medium and the concentrated cells were subsequently transferred to the temperature-controlled MIMS cuvette, which was set to the growth temperature of 3 °C. To assess rates of O_2 production and O_2 uptake in response to irradiance, *C. debilis* and *P. subcurvata* were exposed to irradiances from 35 up to 1425 μmol photons m^{-2} s^{-1} during consecutive light–dark periods as in chlorophyll *a* fluorescence measurements. Light and dark intervals during the assay lasted 10 min to obtain O_2 fluxes under steady-state conditions. Assays were performed under saturating DIC concentrations of ≥2000 μmol L^{-1}. O_2-evolving and O_2-consuming processes were separated in the light by measuring the $^{16}O_2$ evolution from water splitting and $^{18}O_2$ uptake from the medium. Further details on the method and calculations of O_2 fluxes are given in Peltier and Thibault (1985) and Fock and Sültemeyer (1989).

Table 1
Parameters of the seawater carbonate system were calculated from TA, pH, silicate, phosphate, temperature, and salinity using the CO2Sys program (Pierrot et al., 2006).

Target pCO_2	pCO_2	CO_2	DIC	TA	pH
(μatm)	(μatm)	(μmol kg^{-1})	(μmol kg^{-1})	(μmol kg^{-1})	(NBS)
High, 1000	967 ± 66	51 ± 5	2247 ± 38	2308 ± 32	7.77 ± 0.03
Low, 160	159 ± 8	9 ± 0.5	1978 ± 23	2294 ± 15	8.47 ± 0.02

3. Results

3.1. CO_2-dependent chlorophyll a fluorescence

The effective quantum yield F'_q/F'_m generally increased with increasing CO_2 concentrations in all four tested species (Fig. 1A–D), but species were differently affected by the acclimation pCO_2. In high pCO_2-acclimated cells of *F. kerguelensis*, the effective quantum yield was increased compared to low pCO_2-acclimated cells while it was lowered in *P. antarctica* and not altered in *C. debilis* and *P. subcurvata*. These species–specific differences in effective quantum yield were also evident in the rETRs and their responses to increasing CO_2 concentration (Fig. 2A–D). Conversely, NPQ strongly decreased with increasing CO_2 concentration in all species and pCO_2 treatments (Fig. 3A–D). The

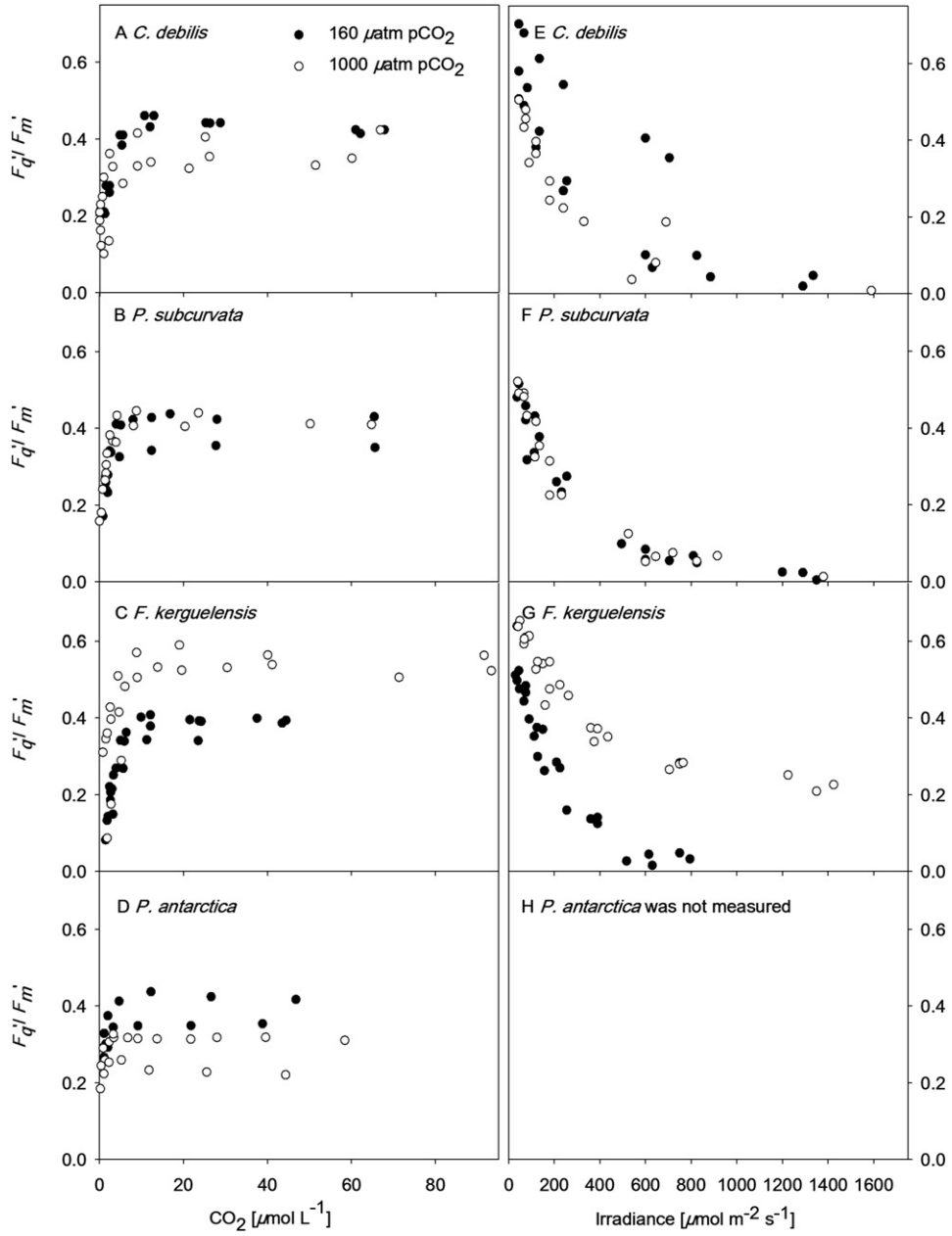

Fig. 1. The effective quantum yield of photochemistry in open reaction centers of PSII (F_q'/F_m') was measured in response to increasing CO_2 concentration (A–D) or irradiance (E–G) in *C. debilis*, *P. subcurvata*, *F. kerguelensis*, and *P. antarctica* acclimated to 160 and 1000 μatm pCO_2. Measurements of each species were conducted with at least three replicates. For *P. antarctica*, no measurements in response to increasing irradiance were carried out. Each data point represents an individual F_q'/F_m' value.

functional absorption cross section of PSII in ambient light (σ'_{PSII}) substantially differed between species and depended on the applied CO_2 concentration as well as the acclimation pCO_2 (Fig. 4A–D). In most of the tested species, σ'_{PSII} slightly increased and leveled off towards high CO_2 concentrations irrespective of the acclimation pCO_2. In *F. kerguelensis*, however, σ'_{PSII} remained constant with values ~100 Å^2 in the low pCO_2 acclimation while values decreased from ~400 to ~300 Å^2 with increasing CO_2 concentrations in the high pCO_2 acclimation. The re-oxidation times of the Q_a acceptors τ_{Qa} and τ'_{Qa} remained unaltered in response to short-term changes in CO_2 concentration and in most species, they were also not affected by the acclimation pCO_2 (Fig. 5A,B). Only in *F. kerguelensis*, high acclimation pCO_2 caused τ_{Qa} and τ'_{Qa} values to decrease (*t*-test: $p < 0.0001$). The connectivity factors p and p' did not change with increasing CO_2 concentrations and were independent of the acclimation pCO_2 in most species (Fig. 6A,B). The acclimation pCO_2 only had an effect in *F. kerguelensis*, decreasing p from 0.17 ± 0.03 to 0.07 ± 0.03 in low to high pCO_2- acclimated cells (*t*-test: $p < 0.0001$). With the exception of *P. antarctica* and the high pCO_2-acclimated cells of *F. kerguelensis*, dark exposure generally led to higher values (i.e. $p > p'$).

3.2. Light-dependent chlorophyll a fluorescence

The effective quantum yield decreased with increasing irradiance in the three investigated species (Fig. 1E–G). Even though this general pattern could be observed in both pCO_2 acclimations, in high pCO_2-acclimated cells of *F. kerguelensis* F_q'/F_m' values remained consistently higher. Species–specific differences in the light-dependence of F_q'/F_m' were also reflected in the rETRs (Fig. 2E–G). In *C. debilis* and *P. subcurvata*, rETRs increased until 500 μmol photons m^{-2} s^{-1} and declined at higher irradiances in both pCO_2 acclimations. In *F. kerguelensis*, however, rETR decreased beyond irradiances of 300 μmol photons m^{-2} s^{-1} in the low

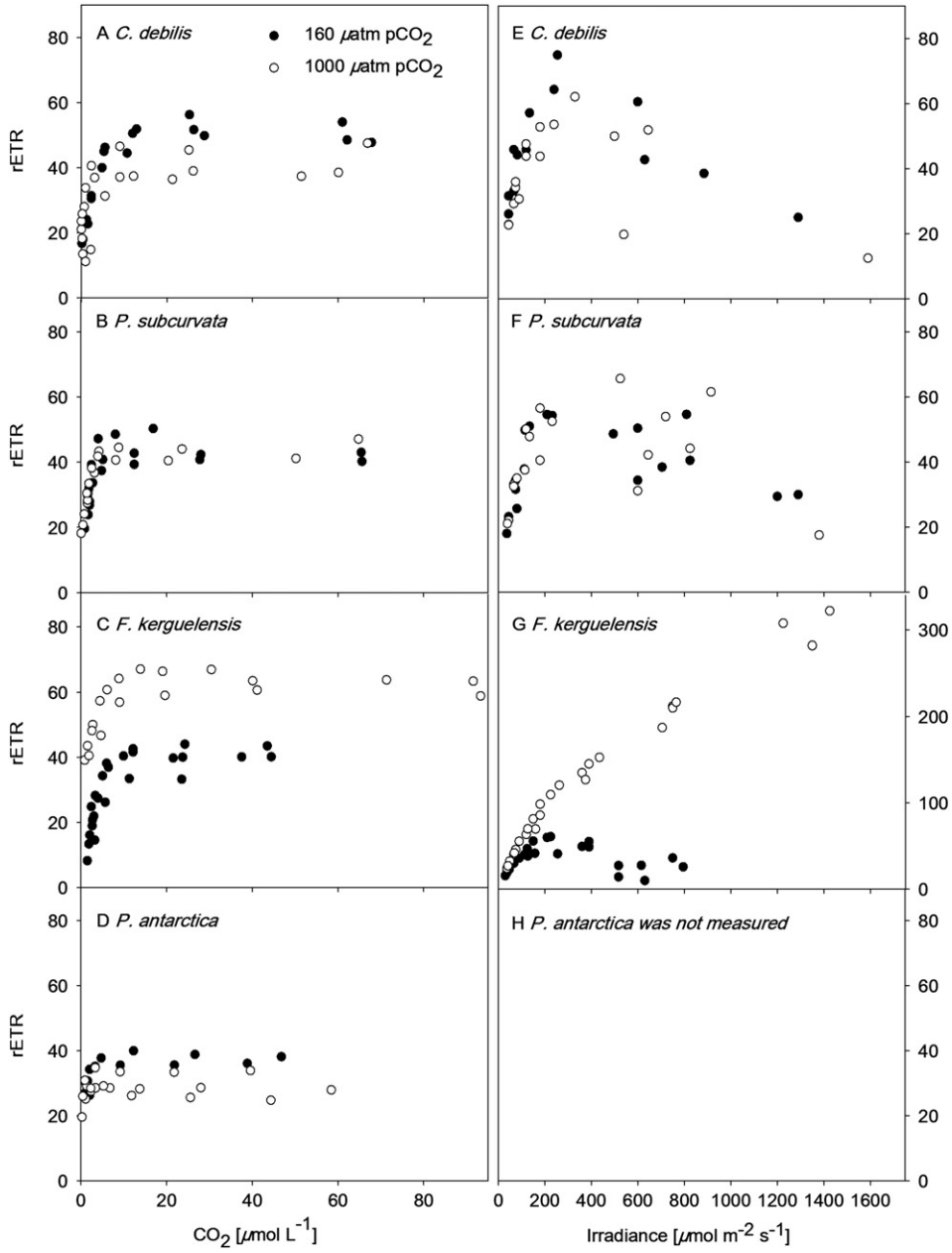

Fig. 2. Relative electron transport rates (rETRs) were determined in response to increasing CO_2 concentration (A–D) or irradiance (E–G) in *C. debilis*, *P. subcurvata*, *F. kerguelensis*, and *P. antarctica* acclimated to 160 and 1000 µatm pCO_2. Measurements of each species were conducted with at least three replicates. For *P. antarctica*, no measurements in response to increasing irradiance were carried out. rETRs were obtained in at least three individual measurements. Each data point represents an individual rETR value.

pCO_2 acclimation while they continued to increase over the entire tested light range in the high pCO_2 acclimation. In all species, NPQ went up from 0 to ~2 when increasing irradiance levels were applied and there was no effect of the acclimation pCO_2 (Fig. 3E–G). The observed responses in σ'_{PSII} differed among species (Fig. 4E–G). For *C. debilis* and *P. subcurvata*, σ'_{PSII} values slightly decreased until irradiances of up to 500 µmol photons m^{-2} s^{-1} and remained more or less constant at higher irradiances independent of the acclimation pCO_2. In contrast, the acclimation pCO_2 led to contrasting responses in *F. kerguelensis* (Fig. 4G), where σ'_{PSII} was ~142 $Å^2$ in the low pCO_2 acclimation, but increased up to ~430 $Å^2$ with increasing irradiance in the high pCO_2 acclimation. Neither τ_{Qa} nor τ'_{Qa} changed in response to short-term changes in irradiance in all species (Fig. 5C,D). In contrast to *C. debilis* and *P. subcurvata*, in which the acclimation pCO_2 did not affect τ_{Qa} and τ'_{Qa} (*t*-test: $p > 0.05$), both parameters were significantly reduced in high pCO_2-acclimated cells of *F. kerguelensis* (*t*-test: $p < 0.0001$). Generally, dark-adapted τ_{Qa} rates were higher than the light-adapted τ'_{Qa}rates. The connectivity factors p and p' remained unaltered by the applied short-term changes in irradiance in the tested species (Fig. 6C,D). In most cases, p values were higher than p' values (Fig. 6C,D). Only in *F. kerguelensis*, p values were significantly reduced in the high compared to the low pCO_2 treatment (*t*-test: $p < 0.0001$).

3.3. Light-dependent photosynthetic O_2 evolution and O_2 uptake

Gross O_2 evolution rates were generally not affected by the acclimation pCO_2 in *C. debilis* and *P. subcurvata* (Table 2, *t*-test: $p > 0.05$). Only in *C. debilis* measured at growth light intensity, gross O_2 evolution rates were lower in the high pCO_2 acclimation (*t*-test: $p < 0.05$). Gross O_2 evolution rates were generally enhanced under high light conditions (*t*-test: $p < 0.05$), except for the low pCO_2 treatment of *C. debilis* (*t*-test: $p > 0.05$). Net O_2 evolution rates were not affected by acclimation pCO_2

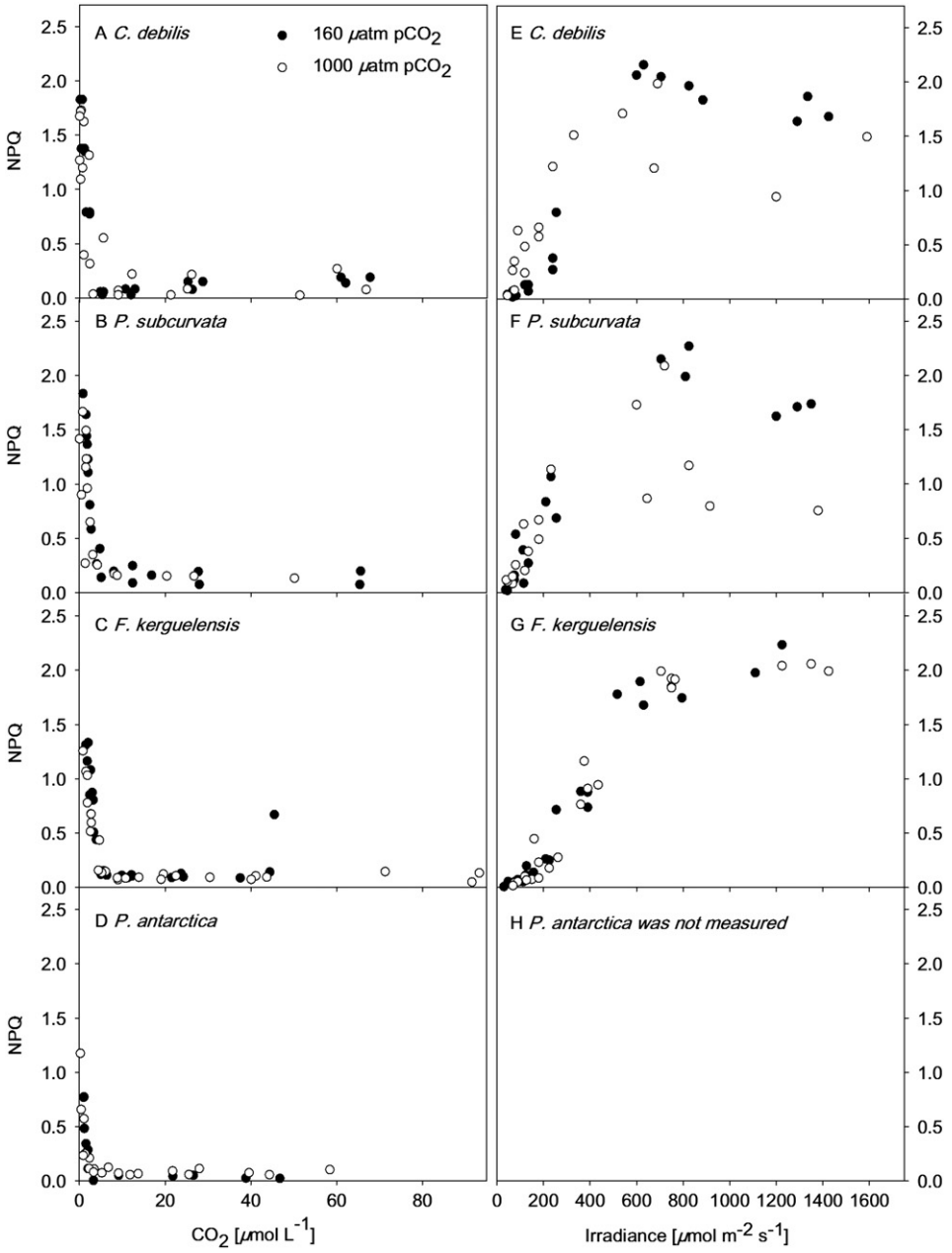

Fig. 3. Non-photochemical quenching (NPQ) was determined in response to increasing CO_2 concentration (A–D) or irradiance (E–G) in *C. debilis*, *P. subcurvata*, *F. kerguelensis*, and *P. antarctica* acclimated to 160 and 1000 µatm pCO_2. Measurements of each species were conducted with at least three replicates. For *P. antarctica*, no measurements in response to increasing irradiance were carried out. Each data point represents an individual NPQ value.

or short-term changes in light in *P. subcurvata* (Table 2, *t*-test: $p > 0.05$) while rates were increased by high light in high CO_2-acclimated cells of *C. debilis* (*t*-test: $p < 0.05$). Values for O_2 uptake in the light were similarly high to those determined in the dark in both tested species (Table 2, *t*-test: $p > 0.05$). In *C. debilis*, O_2 uptake rates in the light as well as in the dark were lower in high pCO_2-acclimated cells irrespective of short-term changes in irradiance (*t*-test: $p < 0.05$). A similar trend was observed for *P. subcurvata* under high light, but not at the light intensity of the acclimation.

4. Discussion

4.1. CO_2-dependent chlorophyll a fluorescence

The F'_q/F'_m measures the efficiency of PSII photochemistry in the light and therefore can be taken as an indication of overall photosynthesis (Genty et al., 1989). Different to the dark-acclimated F_v/F_m, which reflects only processes acting on PSII reaction centers, the light-acclimated F'_q/F'_m also integrates all the processes downstream of PSII. These processes include the redox state of the PQ-pool and the amount of NPQ associated with dynamic and chronic photoinhibition. In our experiments, F'_q/F'_m and rETR were found to increase with increasing CO_2 concentrations in all four tested species (Figs. 1A–D, 2A–D), suggesting that under very low CO_2 concentrations (0–5 µmol L^{-1}) electron transport was mainly limited by the Calvin cycle. In line with this, NPQ was highest under these very low CO_2 concentrations and leveled off at CO_2 concentrations higher than ~5 µmol L^{-1} in all species (Fig. 3A–D). Hence, quenching processes such as xanthophyll cycling prevented the damage of PSII under very low CO_2 concentrations in the tested species. Evidence for high xanthophyll cycle activity has been previously reported in different polar diatom species and the haptophyte *P. antarctica* under high irradiance (Kropuenske et al., 2009; Van Leuwe et al., 2005)

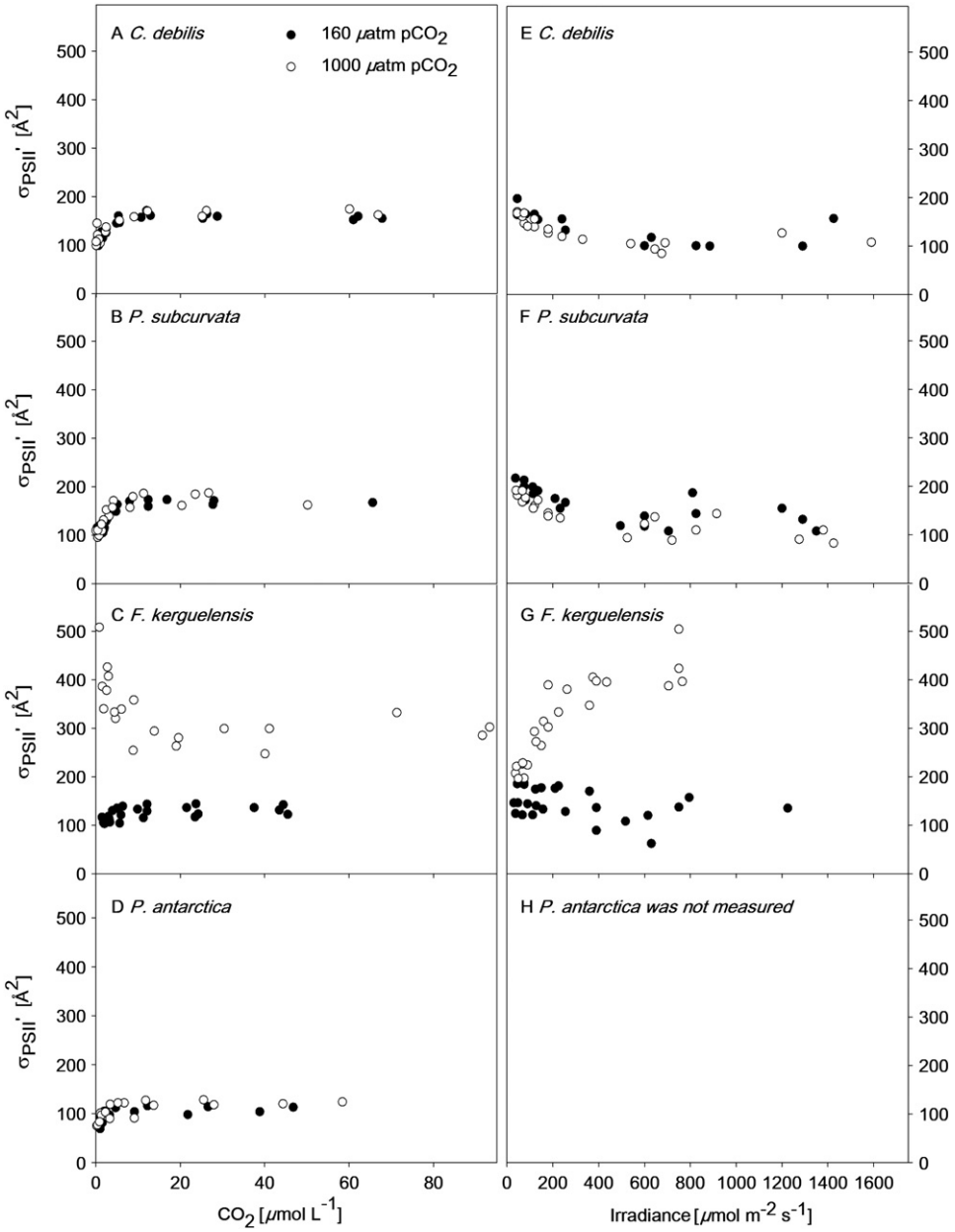

Fig. 4. The functional absorption cross section of PSII (σ_{PSII}') was determined in response to increasing CO_2 concentration (A–D) or irradiance (E–G) in *C. debilis*, *P. subcurvata*, *F. kerguelensis*, and *P. antarctica* acclimated to 160 and 1000 µatm pCO_2. Measurements of each species were conducted with at least three replicates. For *P. antarctica*, no measurements in response to increasing irradiance were carried out. Each data point represents an individual σ_{PSII}' value.

and nutrient limitation (Alderkamp et al., 2012; Petrou et al., 2012), but not yet under low CO_2 concentration.

In parallel to xanthophyll-cycle activity, changes in functional absorption cross section in ambient light σ_{PSII}' reflect changes in the efficiency of exciton delivery to the reaction centers (Olaizola and Yamamoto, 1994) and thus may also play a role in photoprotection. The functional absorption cross section σ_{PSII} describes the functional 'target area' of the light harvesting antenna and is energetically coupled to the O_2-evolving reaction centers (Falkowski and Raven, 2007; Mauzerall and Greenbaum, 1989). Values for σ_{PSII} estimated in our study (mean 171 ± 28 Å^2) match previously published values for phytoplankton (Suggett et al., 2009; Yang and Gao, 2012). In response to high irradiance, σ_{PSII}' was found to be highly variable, suggesting that the antenna quenching contributes to photoprotection (Falkowski et al., 1994; Gorbunov et al., 2001; Vassiliev et al., 1994). In our experiments, σ_{PSII}' generally increased slightly and leveled off towards higher CO_2 concentrations apart from high pCO_2-acclimated cells of *F. kerguelensis* (Fig. 4A–D). We suggest that at low CO_2 concentrations applied in the assay, lower σ_{PSII}' could reduce light capture efficiency and accompany NPQ in photoprotection under these conditions.

Among the tested species, acclimation pCO_2 altered photophysiological responses only in *F. kerguelensis*. In this species, F_q'/F_m', rETR and σ_{PSII}' values were enhanced in high pCO_2-acclimated cells (Fig. 1C, 2C, 4C). In line with this, τ_{Qa}' and τ_{Qa} values were lowest in this treatment (Fig. 5A,B), indicating very short re-oxidation times of the Q_a-pool for *F. kerguelensis*. Note that applied changes in CO_2 concentration or irradiance did not alter τ_{Qa}' and τ_{Qa} in any of the tested species (Fig. 5). Consequently, the mean values are also representative for the phytoplankton cell's response during acclimation. The observed shorter Q_a-re-oxidation rates in high pCO_2-acclimated *F. kerguelensis* suggest that the cells relied on additional electron acceptors next to the Calvin cycle, e.g. photorespiration and/or the Mehler reaction. Unfortunately,

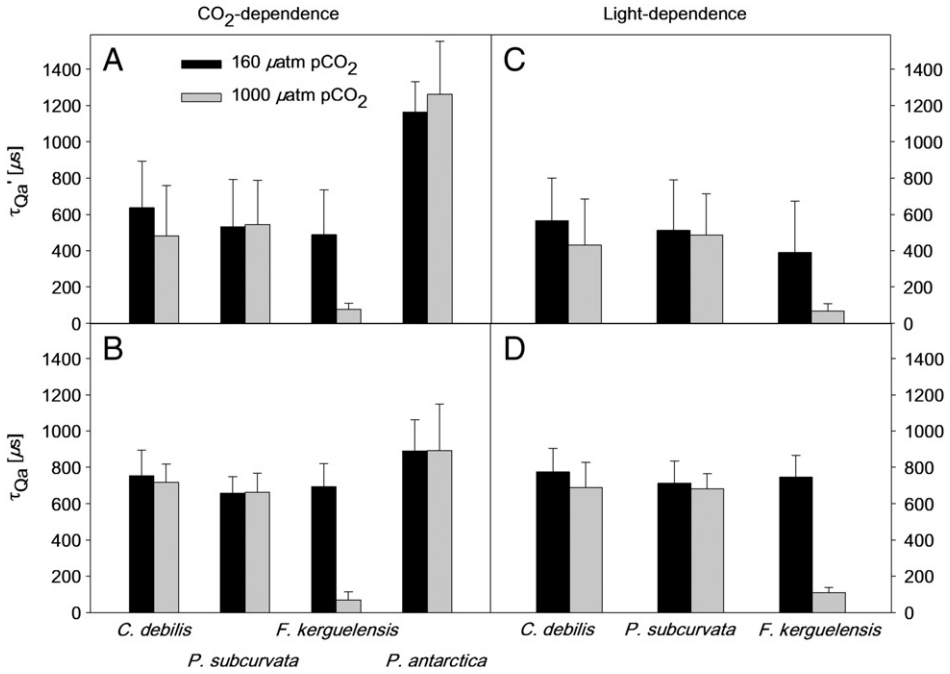

Fig. 5. The time constant for electron transport on the acceptor side of PSII τ_{Qa} and τ_{Qa}' was determined in response to increasing CO_2 concentration or irradiance in *C. debilis*, *P. subcurvata*, *F. kerguelensis*, and *P. antarctica* acclimated to 160 and 1000 µatm pCO_2. Measurements of each species were conducted with at least three replicates. For *P. antarctica*, no measurements in response to increasing irradiance were carried out. As values of τ_{Qa} and τ_{Qa}' did not differ in response to short-term changes in CO_2 concentration (A,B) or irradiance (C,D), mean values of the respective treatments are shown.

O_2 fluxes were not determined and thus no conclusive answer on the presence of the Mehler reaction can be provided for this species. It has also been shown that when the Calvin cycle is saturated through excess irradiance, plastid terminal oxidases can act as energy sinks as these can be active in the light and receive electrons from the plastoquinol (Grouneva et al., 2011; Mackey et al., 2008). Whether this process applies for the tested *F. kerguelensis* remains to be tested.

4.2. Light-dependent chlorophyll a fluorescence

Chlorophyll *a* fluorescence was assessed under saturating DIC supply (≥2000 µM) as a function of irradiance in *C. debilis*, *P. subcurvata* and *F. kerguelensis*. In *C. debilis* and *P. subcurvata*, F_q'/F_m' decreased with increasing irradiance (Fig. 1E,F). When irradiances above 400 µmol photons m^{-2} s^{-1} were applied, F_q'/F_m' went below 0.2 and approached

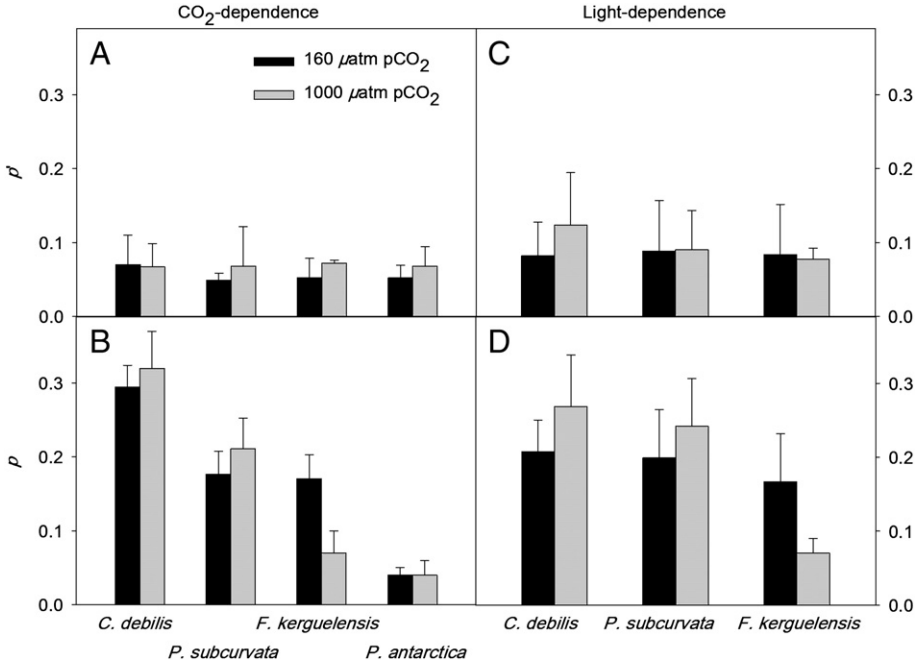

Fig. 6. The connectivity factors *p* and *p′* were determined in response to increasing CO_2 concentration or irradiance in *C. debilis*, *P. subcurvata*, *F. kerguelensis*, and *P. antarctica* acclimated to 160 and 1000 µatm pCO_2. Measurements of each species were conducted with at least three replicates. For *P. antarctica*, no measurements in response to increasing irradiance were carried out. As values of *p* and *p′* did not differ in response to short-term changes in CO_2 concentration (A,B) or irradiance (C,D), mean values of the respective treatments are shown.

Table 2
O_2 fluxes were determined at growth light intensity (90 μmol photons m^{-2} s^{-1}) and high light (>200–1425 μmol photons m^{-2} s^{-1}) under saturating DIC concentrations in *C. debilis* and *P. subcurvata* that were acclimated to 160 and 1000 μatm pCO_2. O_2 fluxes were derived from at least three independent measurements. Values for O_2 evolution and uptake are given in μmol O_2 (mg Chl *a*)$^{-1}$ h^{-1}.

pCO_2 and light intensity	Gross O_2 evolution	Net O_2 evolution	O_2 uptake in the light	O_2 uptake in the dark
C. debilis				
160 μatm at 90 μE	290 ± 28	107 ± 39	203 ± 33	158 ± 56
1000 μatm at 90 μE	205 ± 26	123 ± 15	82 ± 15	64 ± 10
160 μatm under high light	305 ± 34	171 ± 42	149 ± 41	136 ± 44
1000 μatm under high light	293 ± 41	187 ± 24	75 ± 15	71 ± 15
P. subcurvata				
160 μatm at 90 μE	248 ± 13	188 ± 53	60 ± 15	69 ± 13
1000 μatm at 90 μE	236 ± 31	167 ± 19	74 ± 13	79 ± 11
160 μatm under high light	352 ± 39	188 ± 33	178 ± 31	171 ± 33
1000 μatm under high light	312 ± 30	215 ± 31	93 ± 16	90 ± 20

0 when exposed to irradiances higher than 800 μmol photons m^{-2} s^{-1}. Congruently, rETR increased until ~400 μmol photons m^{-2} s^{-1}, but declined in response to higher irradiance indicating photoinhibition in *C. debilis* and *P. subcurvata* (Fig. 2E,F). This response was observed independent of the acclimation pCO_2 in both species. Our results indicate that the short-term exposure to high irradiance induced photoinhibition to a similar degree in both high and low pCO_2-acclimated cells of *C. debilis* and *P. subcurvata*. Evidence for dynamic photoinhibition was provided as the lowered yield under high irradiances during the assay (Fig. 1E,F) fully recovered within 10 min of dark acclimation (data not shown). Dynamic photoinhibition serves as a protection mechanism on time scales between tens of minutes to several hours and is based on the recovery of PSII reaction center proteins (Falkowski et al., 1994). In contrast, the acclimation to low and high pCO_2 led to different photophysiological responses in *F. kerguelensis*. While trends in F_q'/F_m' and rETR of low pCO_2-acclimated cells of *F. kerguelensis* resembled light-dependent responses of *C. debilis* and *P. subcurvata*, responses of the high pCO_2-acclimated *F. kerguelensis* were very different (1E–G, 2E–G). In this treatment, F_q'/F_m' values decreased until values of ~0.3 and remained unaltered at irradiance above 400 μmol photons m^{-2} s^{-1}, indicating the ability to maintain efficient photochemistry despite high irradiances. In line with this, rETRs increased with increasing irradiance levels in high pCO_2-acclimated cells of *F. kerguelensis*, showing no sign of saturation over the investigated light range. We suggest that higher rETRs were enabled in this species because of higher fixation rates by RubisCO at elevated pCO_2. A similar conclusion was drawn by Ihnken et al. (2011a, 2011b), who found enhanced rETRs in high CO_2-acclimated cells of the temperate diatom *C. muelleri*. Interestingly, such a response was not observed in our tested *Chaetoceros* species that manifested signs of dynamic photoinhibition independent of the acclimation pCO_2. It appears that strong species–specific responses exist regarding the susceptibility to photoinhibition in relation to the acclimation pCO_2. While we found evidence for photoinhibition in most of the tested SO diatoms irrespective of the acclimation pCO_2, other studies reported a higher susceptibility to photoinhibition only in the high pCO_2 acclimation of natural phytoplankton assemblages of the China Sea (Gao et al., 2012) as well as in high pCO_2-acclimated cells of the two diatoms *Phaeodactylum tricornutum* (Wu et al., 2010) and *T. pseudonana* (McCarthy et al., 2012). Even for the same strain of *T. pseudonana*, it was also observed that both high and low pCO_2-acclimated cells showed photoinhibition after 40 min exposure to high irradiances while the short-term exposure to high irradiances did not affect rETRs (Yang and Gao, 2012).

Reasons for a different susceptibility of phytoplankton to photoinhibition rely on the cell's ability to prevent photodamage. Under high light conditions, the Calvin cycle can represent the limiting step in photosynthesis (Sukenik et al., 1987) and phytoplankton cells generally rely on xanthophyll cycle-dependent NPQ to dissipate the excess energy. In the three tested species, NPQ increased until an irradiance of ~600 μmol photons m^{-2} s^{-1} and remained high in response to even higher irradiance levels (Fig. 3E–G). Even though all species showed high NPQ, photoprotection strategies in the tested species varied. While under short-term exposure to low light levels σ'_{PSII} was high to ensure efficient light capture in *C. debilis* and *P. subcurvata*, under high light σ'_{PSII} was lowered to diminish incoming light and therewith damage of the photosystems (Fig. 4E,F). Note that acclimation pCO_2 did not affect σ'_{PSII} in these two species. Hence, we conclude that next to xanthophyll cycle-dependent NPQ also changes in σ'_{PSII} contributed to photoprotection in *C. debilis* and *P. subcurvata*, yet these processes were insensitive to the acclimation pCO_2. In *F. kerguelensis*, however, σ'_{PSII} strongly increased with increasing irradiance in high pCO_2-acclimated cells while σ'_{PSII} remained unaltered in response to the applied irradiance levels in low pCO_2-acclimated cells (Fig. 4G). It seems that this species enhances its light capture efficiency, a finding that is in line with the increased rETRs under these conditions (Fig. 2G). Both observations can be explained by the very short re-oxidation times of the Q_a pool observed in high pCO_2-acclimated cells (Fig 5C,D). In comparison, re-oxidation rates were slower in *C. debilis* and *P. subcurvata* irrespective of the acclimation pCO_2. Considering further that high pCO_2-acclimated cells of *F. kerguelensis* were not susceptible to photoinhibition (Fig. 2G), we suggest that the faster Q_a re-oxidation was likely the predominant means for photoprotection in this species.

4.3. The impact of changes in connectivity on photoprotection

Next to changes in σ'_{PSII} and re-oxidation times of the Q_a pool, the connectivity factor *p*, which describes the fraction of energetically connected PSII centers and the migration of excitation energy from closed to open PSII (Blankenship, 2002), provides information on how efficient excitons are redistributed among PSII, thus protecting PSII reaction centers from excess energy flux. Two limiting cases of PSII connectivity can be distinguished. When *p* is equal to zero, each reaction center has its own independent antenna system, implying energetic segregation of the units in the thylakoid membrane. In this case, termed as the 'separate unit' model, each PSII center receives energy from its most adjacent light-harvesting complex (Blankenship, 2002). At the other extreme, a large number of reaction centers are embedded in a common matrix of antenna. In this so-called the 'lake' model, the PSII centers are energetically connected as a large number of open reaction centers share the excitons in the pigment matrix (Blankenship, 2002). The energy transfer between PSII units can be assessed using FIRe. Before discussing our results from chlorophyll *a* fluorescence measurements, we first will theoretically assess how changes in connectivity can affect photosynthetic electron transport rate and thus the build-up of the ΔpH gradient to promote NPQ activation. Using the photosynthetic model of Kroon and Thoms (2006), the time-dependent electron transport rate (ETR) can be calculated using the photochemical yield of PSII (Φ_{PSII}) after Lavergne and Trissl (1995), which is multiplied by the optical cross section for PSII (a^*_{PSII}) and the irradiance (PFD, in μmol quanta m^{-2} s^{-1}):

$$ETR = \Phi_{PSII} a^*_{PSII} PFD cf, \quad (1)$$

where cf is a conversion factor (6.02×10^{14}) to convert units (μmol to quanta, seconds to milliseconds). Using the exciton-radical-pair model of Lavergne and Trissl (1995), Φ_{PSII} can be calculated as follows:

$$\Phi_{PSII} = \Phi^m_{PSII} \frac{(1+J)q}{1+Jq}, \quad (2)$$

where Φ^m_{PSII} is the maximum quantum yield of photochemistry in PSII at the overall fraction of open PSII units $q = 1$. Note that Φ^m_{PSII}, which is calculated with the exciton-radical-pair model by Lavergne and Trissl (1995), deviates from F_v/F_m by Genty et al. (1989) by a factor: $F_v/F_m = 0.87 \times \Phi^m_{PSII}$. Consequently, Eqs. (1) and (2) can be applied to

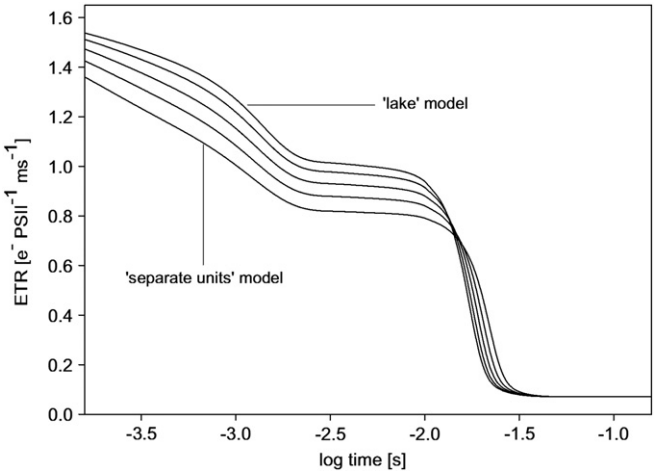

Fig. 7. Theoretical simulations of the photosynthetic electron transport rate (ETR) during a dark–light transient based on the model of Kroon and Thoms (2006). The simulations are based on antenna scenario 2 in Kroon and Thoms (2006) and a high irradiance of 1000 μmol photons m^{-2} s^{-1}. The curves for the induction of the electron transport are calculated for different connectivity parameters *J*, which is directly related to the connectivity parameter *p* (Joliot and Joliot, 1964). The *J* values (from 'separate units' to 'lake' model) are 0, 0.41, 0.92, 1.59, and 2.33.

calculate the impact of connectivity on the photosynthetic electron flow in terms of the parameter *J*, which is related to the connection parameter *p* (Joliot and Joliot, 1964):

$$J = \frac{p}{1-p}. \quad (3)$$

According to the latter equation, the parameter *J* can assume any value between zero and infinity (*J* tends to infinity as *p* approaches 1). In reality, however, the exciton transfer between connected units competes with de-excitation and *J* is restricted to finite values. For a typical antenna size (see Table 2, scenario 2 in Kroon and Thoms (2006)), the calculated *J* can assume any value between zero and 2.33 and thus *p* is restricted to values below about 0.7. The theoretical curves for the induction of the electron transport for various *J* values during a dark–light transient are shown in Fig. 7. While steady state ETRs remained unaffected by a change in *J*, at the beginning of the light phase ETR values were substantially controlled by *J*. Higher values of *J*, as in the 'lake' model, also led to higher ETRs. In comparison, low *J* values as in the 'separate unit' model resulted in lower ETRs (Fig. 7). These results suggest that a high connectivity between PSII can help to increase dissipation of excess energy by electron transport. This might be of particular relevance at the transition from dark to light as then high ETRs can accelerate the build-up of the ΔpH gradient to promote NPQ activation. Hence, we conclude that a high connectivity between PSII might be responsive to quickly induce photoprotection (i.e. NPQ).

These theoretical simulations suggest that changes in connectivity can have the potential to affect ETRs and therewith the induction of NPQ. By means of FIRe measurements, we were able to assess the effect of short-term changes in CO_2 concentration or irradiance on the connectivity *p* in low and high-pCO_2 acclimated cells of the four tested species. We found that short-term changes in CO_2 concentration (Fig. 6A,B) or irradiance (Fig. 6C,D) did not affect *p′* and *p* in the tested species. As expected, we only observed a change in connectivity during dark–light transitions (Fig. 6). Such changes in connectivity were also found in the temperate chlorophyte *Dunaliella tertiolecta* in response to dark–light transitions (Ihnken et al., 2011a, 2011b). In our experiments, *p′* values determined at the end of the light phase were below 0.1 in all tested species (Fig. 6A,C). After transfer to darkness for 10 min, values varied strongly among the tested species. While *p* values were high in *C. debilis* (~0.3) and *P. subcurvata* (~0.2), values were very low in *P. antarctica* (~0.05; Fig. 6B,D). High *p* values recorded at the end of the dark phase reflect a high potential of migration of excitation energy between PSII reaction centers as in the 'lake' model. Our results suggest that in contrast to *P. antarctica*, *C. debilis* and *P. subcurvata* possess energetically well connected PSII reaction centers hinting towards an important role of connectivity in the photoprotection of these species. In the case of *F. kerguelensis*, we additionally observed that *p* was significantly reduced from ~0.2 in low to 0.1 in high pCO_2-acclimated cells (Fig. 6B, D). The strong reduction in *p* was also accompanied by shorter Q_a re-oxidation rates in this treatment (Fig. 5). We therefore conclude that processes such as the Q_a re-oxidation are important to prevent photodamage in *F. kerguelensis* under high pCO_2 while changes in connectivity contribute to NPQ in the photoprotection mechanisms of *C. debilis* and *P. subcurvata*.

4.4. Light-dependent photosynthetic O_2 evolution and O_2 uptake

Next to the photosynthetic O_2 evolution at PSII, other processes like the mitochondrial respiration occur simultaneously and therefore hinder the determination of gross photosynthesis (i.e. water splitting). Using the method by Peltier and Thibault (1985), O_2 evolution from water splitting can be differentiated from O_2 uptake. The light-dependence of O_2 fluxes was assessed in *C. debilis* and *P. subcurvata* acclimated to low and high pCO_2. We observed that gross O_2 evolution rates generally remained unaltered by the pCO_2 during acclimation in the two tested species (Table 2). Only in *C. debilis* when tested under acclimation light intensity (90 μmol photons m^{-2} s^{-1}), gross O_2 evolution was lowered by high acclimation pCO_2. Considering that this species showed a stimulation in growth by 63% from low (0.59 d^{-1}) to high (0.96 d^{-1}) pCO_2 (Trimborn et al., 2013), this is a clear indication of an increased energy use efficiency under high pCO_2. The short-term exposure to high light generally stimulated gross O_2 evolution, except for the low pCO_2 treatment of *C. debilis* (Table 2). The presence of the Mehler reaction was assessed by measuring light-dependent O_2 uptake rates in low and high CO_2-acclimated cells of *C. debilis* and *P. subcurvata*. Independent of the pCO_2 during acclimation, O_2 uptake rates in the light equaled rates obtained in the dark in both species and this was also true when cells were exposed to higher irradiances (Table 2). Consequently, the Mehler reaction did not contribute to photoprotection (Raven and Beardall, 1981) in *C. debilis* and *P. subcurvata*.

The acclimation to high pCO_2 affected dark respiration in the two species differently. At acclimation light intensity, dark respiration rates were equally high in both pCO_2-acclimations of *P. subcurvata* while dark respiration decreased by ~60% from low to high pCO_2 in *C. debilis* (Table 2). Apparently, this species benefits from lower energy requirements at high pCO_2 and this further hints towards a shift from oxidative to reductive pathways (Rokitta et al., 2012). In contrast to our findings, experiments with the temperate diatoms *T. pseudonana* and *P. tricornutum* showed that dark respiration increased with increasing pCO_2, indicating a higher energy demand for maintenance of internal acid-base stability (Wu et al., 2010; Yang and Gao, 2012). Altogether, high pCO_2 does not lead to reduced dark respiration in phytoplankton species *per se*. Some species, like *C. debilis*, might benefit from reduced energy requirements and/or a better energy use efficiency for higher growth in high CO_2 conditions, while in others, such as *P. subcurvata*, energy requirements might remain unaffected or even be enhanced as observed in temperate diatoms (Wu et al., 2010; Yang and Gao, 2012). To gain a better understanding how high pCO_2 will affect SO phytoplankton species, future studies should study processes like dark respiration and gross photosynthesis in more detail.

Acknowledgments

This work was supported by the German Science Foundation (TR899) and the European Research Council (ERC) under the European Community's Seventh Framework Programme (FP7/2007–2013)/ERC grant agreement no. [205150]. **[SS]**

References

Alderkamp, A.-C., Kulk, G., Buma, A.G.J., Visser, R.J.W., Van Dijken, G.J., Mills, M.M., Arrigo, K.R., 2012. The effect of iron limitation on the photophysiology of *Phaeocystis antarctica* (Prymnesiophyceae) and *Fragilariopsis cylindrus* (Bacillariophyceae) under dynamic light. J. Phycol. 48, 45–59.

Arrigo, K.R., van Dijken, G.L., Bushinsky, S., 2008. Primary production in the Southern Ocean, 1997–2006. J. Geophys. Res. 113, C08004. http://dx.doi.org/10.1029/2007JC00455.

Arrigo, K.R., Mills, M.M., Kropuenske, L.R., van Dijken, G.L., Alderkamp, A.-C., Robinson, D.H., 2010. Photophysiology in two major Southern Ocean phytoplankton taxa: photosynthesis and growth of *Phaeocystis antarctica* and *Fragilariopsis cylindrus* under different irradiance levels. Integr. Comp. Biol. 50, 950–966.

Blankenship, R.E., 2002. Molecular Mechanisms of Photosynthesis. Blackwell Science, Oxford.

Boelen, P., van de Poll, W.H., van der Strate, H.J., Neven, I.A., Beardall, J., Buma, A.G.J., 2011. Neither elevated nor reduced CO_2 affects the photophysiological performance of the marine Antarctic diatom *Chaetoceros brevis*. J. Exp. Mar. Biol. Ecol. 406, 38–45.

Brewer, P.G., Bradshow, A.L., Williams, R.T., 1986. Measurement of total carbon dioxide and alkalinity in the North Atlantic Ocean in 1981. In: Trabalka, J.R., Reichle, D.E. (Eds.), The Changing Carbon Cycle — a Global Analysis. Springer, New York, pp. 358–381.

Falkowski, P.G., Raven, J.A., 2007. Aquatic Photosynthesis. Princeton University Press, Princeton.

Falkowski, P.G., Greene, R., Kolber, Z., 1994. Light utilization and photoinhibition of photosynthesis in marine phytoplankton. In: Bowyer, J., Baker, N.R. (Eds.), Photoinhibition of Photosynthesis — From Molecular Mechanisms to the Field, Bios Scientific, London, pp. 409–434 (i).

Feely, R.A., Doney, S.C., Cooley, S.R., 2009. Ocean acidification. Present conditions and future changes in a high-CO2 world. Oceanography 22, 36–47 (c, London).

Feng, Y., Hare, C.E., Rose, J.M., Handy, J.M., DiTullio, G.R., Lee, P.A., Smith Jr., W.O., Peloquin, J., Tozzi, S., Sun, J., Zhang, Y., Dunbar, R.B., Long, M.C., Sohst, B., Lohan, M., Hutchins, D.A., 2010. Interactive effects of iron, irradiance and CO_2 on Ross Sea phytoplankton. Deep Sea Res. I 57, 368–383.

Fock, H.P., Sültemeyer, D.F., 1989. O_2 evolution and uptake measurements in plant cells by mass spectrometry. In: Liskens, H.F., Jackson, J.F. (Eds.), Modern Methods of Plant Analysis. Springer, Heidelberg, pp. 3–18.

Gao, K., Xu, J., Gao, G., Li, Y., Hutchins, D.A., Huang, B., Wang, L., Zheng, Y., Jin, P., Cai, X., Häder, D.-P., Li, W., Xu, K., Liu, N., Riebesell, U., 2012. Rising CO_2 and increased light exposure synergistically reduce marine primary productivity. Nat. Clim. Chang. 2, 519–523.

Genty, B., Briantais, J.-M., Baker, N.R., 1989. The relationship between the quantum yield of photosynthetic electron transport and quenching of chlorophyll fluorescence. Biochim. Biophys. Acta 990, 87–92.

Gorbunov, M.Y., Kolber, Z.S., Lesser, M.P., Falkowski, P.G., 2001. Photosynthesis and photoprotection in symbiotic corals. Limnol. Oceanogr. 46, 75–85.

Gran, G., 1952. Determinations of the equivalence point in potentiometric titrations of seawater with hydrochloric acid. Oceanol. Acta 5, 209–218.

Grouneva, I., Rokka, A., Aro, E.-M., 2011. The thylakoid membrane proteome of two marine diatoms outlines both diatom-specific and species-specific features if the photosynthetic machinery. J. Proteome Res. 10, 5338–5353.

Guillard, R.R.L., Ryther, J.H., 1962. Studies of marine planktonic diatoms. Can. J. Microbiol. 8, 229–239.

Hoogstraten, A., Timmermans, K.R., de Baar, H.J.W., 2012a. Morphological and physiological effects in *Proboscia alata* (Bacillariophyceae) grown under different light and CO_2 conditions of the modern Southern Ocean. J. Phycol. 48, 559–568.

Hoogstraten, A., Peters, M., Timmermans, K.R., de Baar, H.J.W., 2012b. Combined effects of inorganic carbon and light on *Phaeocystis globosa* Scherffel (Prymnesiophyceae). Biogeosciences 9, 1885–1896.

Ihnken, S., Roberts, S., Beardall, J., 2011a. Differential responses of growth and photosynthesis in the marine diatom *Chaetoceros muelleri* to CO_2 and light availability. Phycologia 50, 82–193.

Ihnken, S., Kromkamp, J.C., Beardall, J., 2011b. Photoacclimation in *Dunaliella tertiolecta* reveals a unique NPQ pattern upon exposure to irradiance. Photosynth. Res. 110, 123–137.

Intergovernmental panel on climate change, 2007. Working group I report. Climate Change 2007: the Physical Science Basis (http://ipcc-wg1.ucar.edu/wg1/wg1-report.html).

Joliot, P., Joliot, A., 1964. Etudes cinétique de la réaction photochimique libérant l'oxygène au cours de la photosynthèse. C. R. Acad. Sci. Paris 258, 4622–4625.

Kolber, Z.S., Prasil, O., Falkowski, P.G., 1998. Measurements of variable chlorophyll fluorescence using fast repetition rate techniques: defining methodology and experimental protocols. Biochim. Biophys. Acta Bioenerg. 1367, 88–106.

Kranz, S.A., Levitan, O., Richter, K.-U., Prásil, O., Berman-Frank, I., Rost, B., 2010. Combined effects of CO_2 and light on the N_2-fixing cyanobacterium *Trichodesmium* IMS101: physiological responses. Plant Physiol. 154, 334–345.

Kroon, B., Thoms, S., 2006. From electron to biomass: a mechanistic model to describe phytoplankton photosynthesis and steady-state growth rates. J. Phycol. 42, 593–609.

Kropuenske, L.R., Mills, M.M., Van Dijken, G.L., Bailey, S., Robinson, D.H., Welschmeyer, N.A., Arrigo, K.R., 2009. Photophysiology in two major Southern Ocean phytoplankton taxa: photoprotection in *Phaeocystis antarctica* and *Fragilariopsis cylindrus*. Limnol. Oceanogr. 54, 1176–1196.

Kropuenske, L.R., Mills, M.M., Van Dijken, G.L., Alderkamp, A.-C., Berg, G.M., Robinson, D.H., Welschmeyer, N.A., Arrigo, K.R., 2010. Strategies and rates of photoacclimation in two major Southern Ocean phytoplankton taxa: *Phaeocystis antarctica* (Haptophyta) and *Fragilariopsis cylindrus* (Bacillariophyceae). J. Phycol. 46, 1138–1151.

Lavergne, J., Trissl, H.-W., 1995. Theory of fluorescence induction in photosystem II: derivation of analytical expressions in a model including exciton-radical pair equilibrium and restricted energy transfer between photosynthetic units. Biophys. J. 68, 2474–2492.

Mackey, K.R.M., Paytan, A., Grossmann, A.R., Bailey, S., 2008. A photosynthetic strategy for coping in a high-light, low nutrient environment. Limnol. Oceanogr. 53, 900–913.

Mauzerall, D., Greenbaum, N.L., 1989. The absolute size of a photosynthetic unit. Biochim. Biophys. Acta 974, 119–140.

McCarthy, A., Rogers, S.P., Duffy, S.J., Campbell, D.A., 2012. Elevated carbon dioxide differentially alters the photophysiology of *Thalassiosira pseudonana* (Bacillariophyceae) and *Emiliania huxleyi* (Haptophyta). J. Phycol. 48, 635–646.

Mills, M.M., Kropuenske, L.R., van Dijken, G.L., Alderkamp, A.-C., Berg, G.M., Robinson, D.H., Welschmeyer, N.A., Arrigo, K.R., 2010. J. Phycol. 46, 1114–1127.

Olaizola, M., Yamamoto, H.J., 1994. Short-term response of the diadinoxanthin cycle and fluorescence yield to high irradiance in *Chaetoceros muelleri* (Bacillariophyceae). J. Phycol. 30, 606–612.

Orr, J.C., Fabry, V.J., Aumont, O., Bopp, L., Doney, S.C., Feely, R.A., Gnanadesikan, A., Gruber, N., Ishida, A., Joos, F., others, 2005. Anthropogenic acidification over the twenty-first century and its impact on calcifying organisms. Nature 437, 681–686.

Peltier, G., Thibault, P., 1985. O_2 uptake in the light in *Chlamydomonas*. Plant Physiol. 79, 225–230.

Petrou, K., Hill, R., Doblin, M., McMinn, A., Johnson, R., Wright, S., Ralph, P.J., 2011. Photoprotection of sea ice microalgal communities from the East Antarctic pack ice. J. Phycol. 47, 77–86.

Petrou, K., Kranz, S.A., Doblin, M.A., Ralph, P.J., 2012. Photophysiological responses of *Fragilariopsis cylindrus* (Bacillariophyceae) to nitrogen depletion at two temperatures. J. Phycol. 48, 127–136.

Pierrot, D.E., Lewis, E., Wallace, D.W.R., 2006. MS Excel Program Developed for CO_2 System Calculations. Carbon Dioxide Information Analysis Center, Oak Ridge National Laboratory, U.S. Department of Energy (http://cdiac.ornl.gov/ftp/co2sys. Accessed 04 February 2011).

Prasil, O., Kolber, Z., Berry, J.A., Falkowski, P.G., 1996. Cyclic electron flow around photosystem II in vivo. Photosynth. Res. 48, 395–410.

Raven, J.A., Beardall, J., 1981. Respiration and photorespiration. Can. Bull. Fish. Aquat. Sci. 210, 55–82.

Raven, J.A., Lucas, W.J., 1985. Energy costs of carbon acquisition. In: Lucas, W.J., Berry, J.A. (Eds.), Inorganic Carbon Uptake by Aquatic Photosynthetic Organisms. American Society of Plant Physiologists, Rockville, pp. 305–324.

Redfield, A.C., 1958. The biological control of chemical factors in the environment. Am. Sci. 46, 205–222.

Reinfelder, J.R., 2011. Carbon concentrating mechanisms in eukaryotic marine phytoplankton. Annu. Rev. Mar. Sci. 3, 291–315.

Robinson, D.H., Kolber, Z., Sullivan, C.W., 1997. Photophysiology and photoacclimation in surface sea ice algae from McMurdo Sound, Antarctica. Mar. Ecol. Prog. Ser. 147, 243–256.

Rokitta, S.D., John, U., Rost, B., 2012. Ocean acidification affects redox-balance and ion-homeostasis in the life-cycle stages of *Emiliania huxleyi*. PLOS One 7, 1–10.

Sigman, D.M., Hain, M.P., Haug, G.H., 2010. The polar ocean and glacial cycles in atmospheric CO_2 concentration. Nature 466, 47–55.

Spalding, M.H., Critchley, C., Orgren, G., Orgren, W.L., 1984. Influence of carbon-dioxide concentration during growth on fluorescence induction characteristics of the green alga *Chlamydomonas reinhardtii*. Photosynth. Res. 5, 169–176.

Suggett, D.J., Moore, C.M., Hickman, A.E., Geider, R.J., 2009. Interpretation of fast repetition rate (FRR) fluorescence: signatures of phytoplankton community structure versus physiological state. Mar. Ecol. Prog. Ser. 376, 1–19.

Sukenik, A., Bennett, J., Falkowski, P.G., 1987. Light-saturated photosynthesis — limitation by electron-transport or carbon fixation. Biochim. Biophys. Acta 891, 205–215.

Sültemeyer, D., Biehler, K., Fock, H.P., 1993. Evidence for the contribution of pseudocyclic photophosphorylation to the energy requirement of the mechanism for concentrating inorganic carbon in *Chlamydomonas*. Planta 189, 235–242.

Tortell, P.D., Payne, C.D., Li, Y., Trimborn, S., Rost, B., Smith, W.O., Risselman, C., Dunbar, R., Sedwick, P., di Tullio, G.R., 2008. The CO_2 sensitivity of Southern Ocean phytoplankton. Geophys. Res. Lett. 35, L04605. http://dx.doi.org/10.1029/2007GL032583.

Trimborn, S., Brenneis, T., Sweet, E., Rost, B., 2013. Sensitivity of Antarctic phytoplankton species to ocean acidification: growth, carbon acquisition and species interaction. Limnol. Oceanogr. 58, 997–1007.

Van Leuwe, M.A., van Sikkelerus, B., Gieskes, W.W.C., Stefels, J., 2005. Taxon-specific differences in photoacclimation to fluctuating irradiance in an Antarctic diatom and a green flagellate. Mar. Ecol. Prog. Ser. 288, 9–19.

Vassiliev, I.R., Prasil, O., Wyman, K., Kolber, Z., Hanson Jr., A.K., Prentice, J., Falkowski, P.G., 1994. Inhibition of PSII photochemistry by PAR and UV radiation in natural phytoplankton communities. Photosynth. Res. 42, 51–64.

Wu, Y., Gao, K., Riebesell, U., 2010. CO_2-induced seawater acidification affects physiological performance of the marine diatom *Phaeodactylum tricornutum*. Biogeosciences 7, 2915–2923.

Yang, G., Gao, K., 2012. Physiological responses of the marine diatom *Thalassiosira pseudonana* to increased pCO_2 and seawater acidity. Mar. Env. Res. 79, 142–151.